



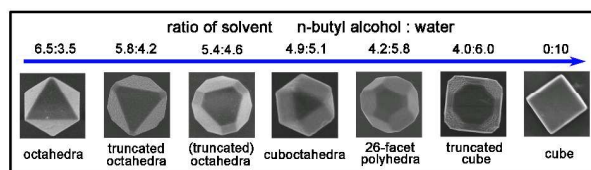
**Microwave-Assisted Synthesis of Cu<sub>2</sub>O Microcrystals with Systematic Shape Evolution from Octahedral to Cubic and Their Comparative Photocatalytic Activities**

Journal:	<i>RSC Advances</i>
Manuscript ID:	RA-ART-05-2014-005015.R1
Article Type:	Paper
Date Submitted by the Author:	25-Jul-2014
Complete List of Authors:	Zhang, Hongdan; Jilin University, State Key Laboratory of Inorganic Synthesis and Preparative Chemistry, College of Chemistry Liu, Fuyang; Jilin University, State Key Laboratory of Inorganic Synthesis and Preparative Chemistry, College of Chemistry Li, Benxian; Jilin University, College of Earth Science Xu, Jiasheng; Bohai University, Chemical Engineering and Food Safety, College of Chemistry Zhao, Xudong; Jilin University, State Key Laboratory of Inorganic Synthesis and Preparative Chemistry, College of Chemistry Liu, Xiaoyang; Jilin University, State Key Lab of Inorganic Synthesis and Preparative Chemistry

# Microwave-Assisted Synthesis of $\text{Cu}_2\text{O}$ Microcrystals with Systematic Shape Evolution from Octahedral to Cubic and Their Comparative Photocatalytic Activities

Hongdan Zhang<sup>1</sup>, Fuyang Liu<sup>1</sup>, Benxian Li<sup>2</sup>, Jiasheng Xu<sup>3</sup> and Xiaoyang Liu<sup>1,2\*</sup>

In this paper, it was firstly realized that the control morphology of  $\text{Cu}_2\text{O}$  under the condition of microwave by simply adjusting the volume ratio of the solvents in reaction medium. Various morphologies of  $\text{Cu}_2\text{O}$  microcrystal, including octahedral, truncated octahedral, cuboctahedral, truncated cubic and cubic microcrystals, were successfully synthesized.



Cite this: DOI: 10.1039/c0xx00000x

www.rsc.org/xxxxxx

ARTICLE TYPE

# Microwave-Assisted Synthesis of Cu<sub>2</sub>O Microcrystals with Systematic Shape Evolution from Octahedral to Cubic and Their Comparative Photocatalytic Activities

Hongdan Zhang<sup>1</sup>, Fuyang Liu<sup>1</sup>, Benxian Li<sup>2</sup>, Jiasheng Xu<sup>3</sup>, Xudong Zhao<sup>1\*</sup> and Xiaoyang Liu<sup>1,2\*</sup>

<sup>5</sup> Received (in XXX, XXX) Xth XXXXXXXXXX 20XX, Accepted Xth XXXXXXXXXX 20XX

DOI: 10.1039/b000000x

Cuprous oxide (Cu<sub>2</sub>O) microcrystals with systematic shape evolution were successfully synthesized via a facile microwave-assisted heating technique. The monodispersed Cu<sub>2</sub>O was synthesized using copper acetate as a starting material, ethylene diamine tetraacetic acid (EDTA) as a reducing agent and surface-regulating agent and the mixture of water and n-butyl alcohol as reaction solvent. Various morphologies of Cu<sub>2</sub>O microcrystal, including octahedral, truncated octahedral, cuboctahedral, truncated cubic and cubic microcrystals, were obtained by altering the volume ratios of n-butyl alcohol to water. The morphologies and optical properties of the synthesized Cu<sub>2</sub>O microcrystals were characterized by XRD, SEM, TEM, HRTEM, SADE and UV-Vis/DRS. The growth mechanism of these crystals was thereby proposed. The volume ratio of n-butyl alcohol to water in the reaction medium was a critical factor to precisely control the morphologies of the microcrystals. Furthermore, their comparative photocatalytic activities for the degradation of methyl orange were tested.

## Introduction

Many properties of an inorganic material are highly dependent on its shape and size. Thus, efforts have been made to control the shape and size of various synthetic inorganic materials by varying synthesis conditions.<sup>1-8</sup> Cuprous oxide (Cu<sub>2</sub>O) is an important P-type semiconductor with a direct band gap of about 2.2 eV. It has attracted extensive attention due to its unique structure rendering its potential applications in solar energy conversion,<sup>9</sup> gas sensing,<sup>10</sup> photocatalytic degradation of organic pollutants,<sup>11-15</sup> and as electrodes of lithium ion batteries.<sup>16</sup> In the past decade, much progress has been made to the shape-controlled synthesis of micro- and nanocrystals of Cu<sub>2</sub>O. For example, Choi et al. prepared Cu<sub>2</sub>O crystals with systematic shape evolution from cubic to octahedral by tuning the deployed electrochemical parameters in their electrodeposition processes.<sup>17-21</sup> Huang et al. synthesized a series of Cu<sub>2</sub>O nanocrystals with systematic shape evolution from cubic to rhombic dodecahedral by varying amounts of reductant for the reaction.<sup>12-15</sup> Yang et al. synthesized the Cu<sub>2</sub>O crystals with different morphologies from cubes to nanospheres with the addition of different amounts of poly vinyl (PVP) during the reaction.<sup>22</sup> These methods require unfavorable

pyrrolidone conditions such as electrodeposition processes, soft templates, toxic reducing agents and/or long reaction time. Therefore, it remains a great challenge to develop a facile, effective and green synthetic method of systematically controlling the shape of Cu<sub>2</sub>O particles.

With increasing interest in renewable energy and energy efficiency in recent years, "green" synthesis techniques have been explored in curbing industrial energy usage and waste.<sup>23</sup> As a quick, facile, uniform, energy efficient and green heating technique, microwave irradiation has been widely applied in the syntheses of various products.<sup>24-29</sup> Compared with conventional heating techniques, microwave heating is a promising rapid volumetric heating technique, which can increase reaction rate and shorten reaction time. Despite its wide applications in synthetic chemistry, microwave heating was mostly used to control the morphologies of the products.<sup>30-32</sup>

Determination of structural symmetry and growth behavior of crystals is necessary to effectively control their shapes and sizes. It is known that the growth of inorganic crystals is determined by the relative order of its surface energies under equilibrium conditions.<sup>21</sup> The fastest crystal growth occurs in the direction perpendicular to the face with the highest surface energy, by which higher-energy surface area is eliminated and lower-energy surface area increased. Thus, the specific Cu<sub>2</sub>O facets can be passivated by controlling the thermodynamics and kinetics of nucleation and crystal growth. The shape and size of Cu<sub>2</sub>O particles can be controlled through adjusting the growth velocity order of the Cu<sub>2</sub>O facets. All these can be realized by controlling the experimental conditions.<sup>33-34</sup> The heating efficiency of reactants or the reaction medium is one of the factors that

1. State Key Laboratory of Inorganic Synthesis and Preparative Chemistry, College of Chemistry, Jilin University, 2699 Qianjin Street, Changchun 130012, P. R. China.

2. College of Earth Science, Jilin University, Changchun 130061, P. R. China.

3. College of Chemistry, Chemical Engineering and Food Safety, Bohai University, 19 Sci-tech Road, Jinzhou 121013, P.R. China.

Fax: (+86) 431-85168316; Tel: (+86) 431-85168316 E-mail: liuxy@jlu.edu.cn

For ESI and other electronic format see DOI: 10.1039/b000000x

influence the growth rates in different crystal directions. Therefore, the dielectric properties of the reaction medium, such as a specific material or solvent, should be considered under microwave irradiation. It has been proven that a reaction medium with high dielectric loss ( $\delta$ ) at the standard operating frequency of a microwave reactor (2.45 GHz), corresponds to higher efficiency under microwave irradiation.<sup>35-36</sup> In this work, water and n-butyl alcohol, with different dielectric constants of 78.4 and 17.5 at 25 °C respectively, were selected as the reaction solvent for the synthesis of Cu<sub>2</sub>O microcrystals.

Herein, micro- and nanocrystals of Cu<sub>2</sub>O with various morphologies were synthesized using microwave heating. A series of monodispersed Cu<sub>2</sub>O microcrystals with various morphologies, including octahedra, truncated octahedra, cuboctahedra, truncated cubes and cubes were obtained by varying the volume ratios of n-butyl alcohol to water in the reaction solvent. The growth mechanism of these Cu<sub>2</sub>O microcrystals was proposed based on the electron microscopy (SEM) analysis. The photocatalytic activities of the as-synthesized Cu<sub>2</sub>O microcrystals were also analyzed using methyl orange (MO) as a substrate. This work not only improves existing synthesis pathways of Cu<sub>2</sub>O microcrystals, but also opens up a new synthesis pathway for facile production of Cu<sub>2</sub>O microcrystal with desired morphology. Morphology control of Cu<sub>2</sub>O crystals under microwave irradiation were for the first time achieved by simply adjusting the volume ratios of the solvents in the reaction medium with no need for surfactants.

## Experimental Section

### Materials and Measurements

All the reagents and solvents for the synthesis were purchased from commercial sources and used as received without further purification. Chemicals used in this study included, Cu(Ac)<sub>2</sub>·2H<sub>2</sub>O (99.5 %, Guangdong Xilong Co., China), EDTANa<sub>2</sub>·2H<sub>2</sub>O (99.0 %, Nanjing Chemical Company, China), NaOH (96 %, Beijing Co., China), n-butyl alcohol (99.5 %, Nanjing Chemical Company, China), and ethanol (AR, Beijing Fine Chemical Company, China).

The resulting phases of the samples were characterized by X-ray diffraction (XRD, Cu K $\alpha$ 1 radiation, Rigaku D/max2550 VB, Japan). The morphologies and structures of samples were analyzed using a scanning electron microscopy (SEM, JSM-6700 F, JEOL, Japan) and transmission electron microscopy (TEM, JSM-3010, JEOL, Japan), respectively. The selected area electron diffraction (SAED) patterns were measured on a JEOL-2010 microscope with an accelerating voltage of 200 kV. A spectrophotometer (Model 2501 PC, Shimadzu) was used to record the UV-Vis diffuse reflectance spectra of the samples. Total organic carbon (TOC) analyzer (Vario TOC cube, Elementar) was employed for the determination of TOC. Methyl orange (C<sub>14</sub>H<sub>14</sub>N<sub>3</sub>NaO<sub>3</sub>S, MO) was used as a model pollutant to investigate the adsorption and photocatalytic activities of the Cu<sub>2</sub>O microcrystals with different shapes. Briefly, 0.025 g Cu<sub>2</sub>O was dispersed in 50 mL of 15 mg/L MO solution and the solution was vigorously stirred in the dark for 6h. The photodegradation process was carried out at room temperature in a double-layer reactor thermostatted with running water. The solution was

irradiated using a 500 W xenon lamp equipped with a filter cutoff of 400 nm. The MO concentration was determined from its UV-Vis absorption at 435 nm.

### Preparation of seven Cu<sub>2</sub>O microcrystals

Seven Cu<sub>2</sub>O microcrystals were prepared and the reaction conditions are listed in Table 1. In a typical synthesis, 0.744 g EDTANa<sub>2</sub>·2H<sub>2</sub>O and 0.32 g NaOH were dissolved in 3.5 mL water followed by the addition of 0.11 g Cu(Ac)<sub>2</sub>·2H<sub>2</sub>O and 6.5 mL n-butyl alcohol. The volumes of water and n-butyl alcohol were altered to produce different microcrystals. After sonication for 30 s, the solution was transferred into a microwave glass vessel. The vessel was then put into a single-mode Microwave Synthesizer (Biotage AB, Sweden) and irradiated for 15 min at 100 °C under magnetic stirring. The final Cu<sub>2</sub>O products were filtered and washed with distilled water and ethanol each for three times.

**Table 1.** Volume ratios of n-butyl alcohol and water in the synthesis of Sample a-g.

No.	N-butyl alcohol (ml)	Water (ml)
a	6.5	3.5
b	5.8	4.2
c	5.4	4.6
d	4.9	5.1
e	4.2	5.8
f	4	6
g	0	10

## Results and discussion

The phase and purity of the as-obtained products were determined by X-ray diffraction (XRD). Fig. 1 shows the XRD patterns of products obtained in an n-butyl alcohol /water solvent with different volume ratios. All the diffraction peaks were indexed using the standard cubic structure of Cu<sub>2</sub>O (lattice constant  $a = 0.427$  nm, JCPDS file No. 05-0667) as a reference. No peaks of impurities such as copper or cupric oxide were detected, suggesting the high purity of the as-obtained products. It was concluded that this method yields impurity-free Cu<sub>2</sub>O. The intensity ratios of (111) to (200) for cubic and octahedral Cu<sub>2</sub>O were 2.9 and 3.8, respectively. The higher (111) diffraction intensity of octahedral Cu<sub>2</sub>O suggests that the surfaces of the octahedral Cu<sub>2</sub>O products have {111} crystal planes. The SEM images of the Cu<sub>2</sub>O microcrystals reveal different morphologies of the crystals prepared in the n-butyl alcohol/water reaction medium with various volume ratios (Fig. 2). The detailed structure of individual Cu<sub>2</sub>O microcrystals particle is shown in

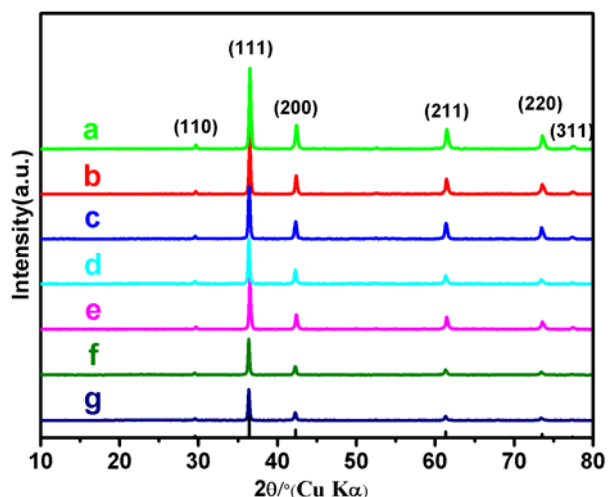
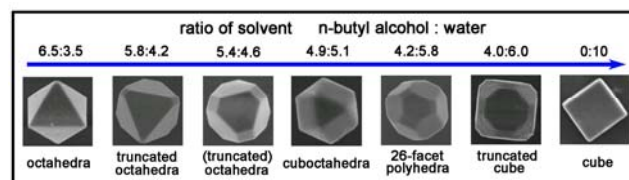


**Figure 1.** Powder X-ray diffraction patterns of the different morphologies of  $\text{Cu}_2\text{O}$  microcrystals. (a) octahedra, (b) type I truncated octahedra, (c) type II truncated octahedra, (d) cuboctahedra, (e) 26-facet polyhedra, (f) truncated cubes, and (g) cubes.

the magnified SEM images. The uniform octahedral  $\text{Cu}_2\text{O}$  microcrystals (sample a) were obtained in a medium of n-butyl alcohol/water at a volume ratio of 6.5: 3.5 as shown in Fig. 2a.  $\text{Cu}_2\text{O}$  microcrystals with 8 truncated triangular faces and 6 square faces were produced when the n-butyl alcohol/water volume ratio decreased to 5.8:4.2 (Fig. 2b). These two shapes had truncated corners from the ideal octahedral structure and denoted as type I truncated octahedra herein. Sample c was prepared in the medium of n-butyl alcohol/water at a volume ratio of 5.4:4.6. The particles had 8 regular hexagonal faces and 6 square faces, which was caused by an increase in the area of {100} facets as shown in Fig. 2c. They are denoted as type II truncated octahedra in this work. Cuboctahedra  $\text{Cu}_2\text{O}$  microcrystals with 8 regular triangular faces and 6 square faces (Sample d) were produced in the n-butyl alcohol/water medium at a volume ratio of 4.9:5.1 as shown in Fig. 2d. Further decreasing n-butyl alcohol/water volume ratio to 4:6 leads to the formation of edge truncated cubes (Sample e) as shown in Fig. 2e. Perfect cubic  $\text{Cu}_2\text{O}$  microparticles (sample f) were obtained in water without any n-butyl alcohol, e.g. at a n-butyl alcohol/water volume ratio of 0:10. Therefore, the morphology control of  $\text{Cu}_2\text{O}$  products was achieved by controlling the volume ratio of n-butyl alcohol to water.

The shape evolution of  $\text{Cu}_2\text{O}$  microcrystals from octahedra to cubes produced by simply varying the volume ratios of n-butyl alcohol and water is illustrated in Scheme 1. The volume ratio of n-butyl alcohol to water present in the reaction medium plays a crucial role in directing the overall morphologies of these intermediate structures. It has been reported that crystal growth behavior is determined by the relative strength of surface energies under equilibrium conditions.<sup>37</sup> The fastest crystal growth occurs in the direction perpendicular to the face with the highest surface energy, by which higher-energy surfaces are eliminated and lower-energy surfaces increased. Many factors may affect the relative surface energies during crystal growing. For example, the presence of chloride ions in the reaction system can selectively lower the surface energy of {100} facets of  $\text{Cu}_2\text{O}$  nanostructure rather than that of its {111} facets. This stabilizes {100} facets and induces the formation of single-crystal nanocubes.<sup>38</sup>



**Scheme 1.** The summary of the influence of different volume ratios of n-butyl alcohol and water on the morphology of as-prepared products.

Moreover, Wang et al. demonstrated that the ratio ( $R$ ) of the growth rates along the  $\langle 100 \rangle$  and  $\langle 111 \rangle$  directions determined the geometrical shape of a crystal.<sup>39</sup> The shape of  $\text{Cu}_2\text{O}$  nanocrystal evolved sequentially from a perfect cube ( $R = 0.58$ ) to a cuboctahedron ( $R = 0.87$ ), a truncated octahedron ( $0.87 < R < 1.73$ ), and finally to a perfect octahedron ( $R = 1.73$ ) with the increase of  $R$ .

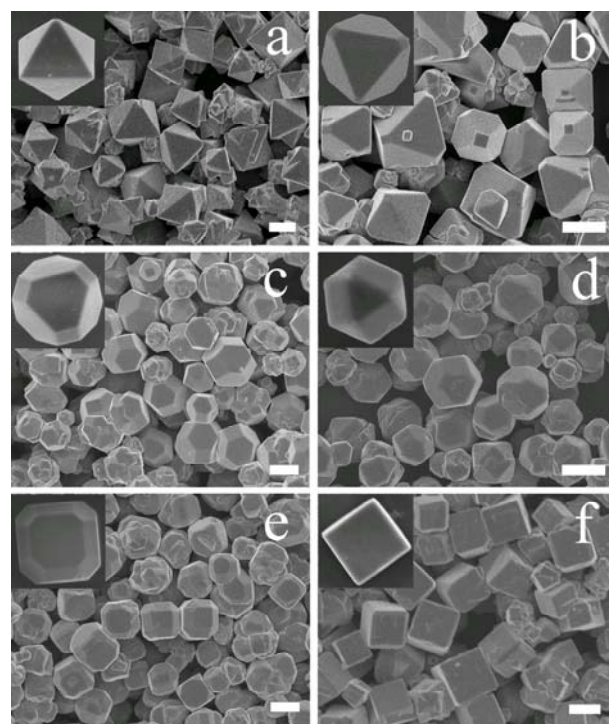


**Figure 2.** SEM images of the  $\text{Cu}_2\text{O}$  microcrystals with various morphologies: (a) octahedra, (b) type I truncated octahedra, (c) type II truncated octahedra, (d) cuboctahedra, (e) truncated cubes, and (f) cubes. Scale bar = 500 nm. Insets show the enlarged views of individual microcrystals.

Microwave heating converts microwave irradiation into thermal energy and the value of the dielectric loss tangent ( $\tan \delta$ ) of the substrate is used as a parameter to evaluate its heating efficiency. Generally, the substance with a larger  $\tan \delta$  exhibits a higher efficiency in converting irradiation energy into heat. The dielectric constants ( $\delta$ ) of water and n-butyl alcohol at 25 °C are 78.4 and 17.5, respectively. Thus, the heating efficiency of the reaction medium increases with the increase of water content due to the higher  $\tan \delta$  value of water. Here, it is assumed that the heating efficiency determines the growth rates in different crystal directions. The growth rate ratio along the  $\langle 100 \rangle$  to  $\langle 111 \rangle$  directions was calculated to be over 1.73 at an n-butyl alcohol/water volume ratio of 6.5:3.5. Thus, octahedral  $\text{Cu}_2\text{O}$  microcrystal was formed with the relatively faster growth of {111}

facets. With the decrease of volume ratio of n-butyl alcohol to water, the growth rate ratio along the  $\langle 100 \rangle$  to  $\langle 111 \rangle$  directions was reduced and the shape of  $\text{Cu}_2\text{O}$  microcrystals evolved in a sequence from octahedron ( $R = 1.73$ ), type I truncated octahedron ( $R = 1.0 < R < 1.73$ ), type II truncated octahedron ( $0.87 < R < 1.15$ ), cuboctahedron ( $R = 0.87$ ), truncated cube ( $0.87 < R < 0.70$ ) and finally to perfect cube ( $R = 0.58$ ).

Fig. 3 shows the TEM images of their relevant SAED patterns and representative SEM images of individual  $\text{Cu}_2\text{O}$  microcrystals with different morphologies. TEM images of the  $\text{Cu}_2\text{O}$  crystals were captured along the  $[111]$  direction of an octahedral crystal (a1), the  $[111]$  directions of a type I truncated octahedral crystal (b1), the  $[100]$  directions of a type II truncated octahedral crystal (c1), and the  $[100]$  direction of a cuboctahedral crystal (d1). The single crystalline nature and sharp faces of these particles can be clearly confirmed in their SEM images.

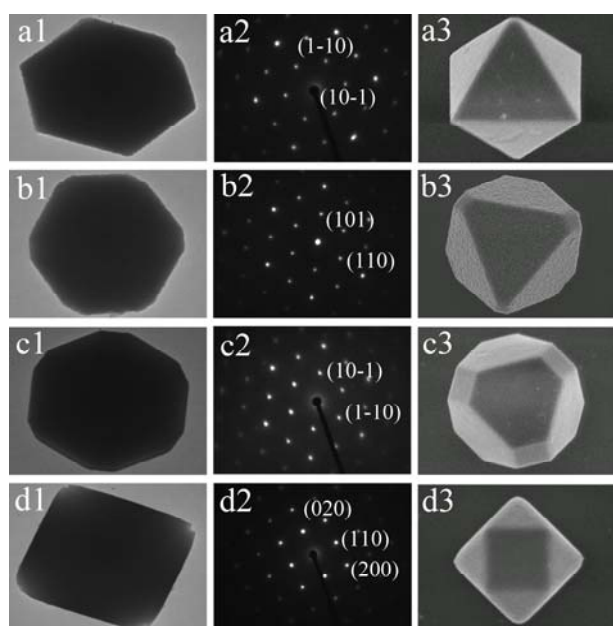


**Figure 3.** TEM images, their corresponding SAED patterns, and representative SEM images of the various morphologies of  $\text{Cu}_2\text{O}$  microcrystals synthesized. TEM images of the  $\text{Cu}_2\text{O}$  crystals viewed along (a1) the  $[111]$  direction of an octahedron, (b1) the  $[111]$  directions of a type I truncated octahedron, (c1) the  $[100]$  directions of a type II truncated octahedron, and (d1) the  $[100]$  direction of a cuboctahedron are shown. Their corresponding SAED patterns are shown along the (a2, b2 and c2)  $[111]$  and (d2)  $[100]$  zone axes of the cuprite crystal.

Fig. S1 shows the UV-vis absorption spectra of  $\text{Cu}_2\text{O}$  products with different morphologies. The absorption spectra of all samples are dominated by strong light scattering bands due to their relatively large sizes. Truncated octahedral  $\text{Cu}_2\text{O}$  crystals showed a strong absorption at 491 nm. Octahedral, truncated cubic and cubic  $\text{Cu}_2\text{O}$  crystals were distinguished by a strong absorption at 501 nm. The calculated band gap energies of these samples are in the range of 2.47-2.52 eV, which is higher than that of bulk  $\text{Cu}_2\text{O}$  (2.17 eV).

The relative adsorption ability and photocatalytic activity of the synthesized  $\text{Cu}_2\text{O}$  microcrystals were investigated using methyl orange (MO) dye as a model. Total concentration of MO was determined by its UV absorption at 455 nm. The absorption spectra of MO solution in the presence of the prepared  $\text{Cu}_2\text{O}$  products indicate that octahedral, truncated octahedral,

cuboctahedra, truncated cubic and cubic  $\text{Cu}_2\text{O}$  microcrystal adsorbed  $\sim 33\%$ ,  $\sim 23\%$ ,  $\sim 16\%$ ,  $\sim 12\%$  and  $\sim 7\%$  of MO, respectively (Fig. 4). The photodegradation of MO vs. time in the presence of the synthesized  $\text{Cu}_2\text{O}$  products are also shown in Fig. 4. After irradiation for 3 h, the percentage of remaining MO in solution in the presence of octahedral, truncated octahedral, cuboctahedral, truncated cubic and cubic  $\text{Cu}_2\text{O}$  microcrystals were 0%, 24%, 72%, 64% and 83%, respectively. The corresponding adsorption spectra and photocatalytic activity of octahedral, truncated octahedral, cuboctahedral, truncated cubic and cubic  $\text{Cu}_2\text{O}$  microcrystals are shown in Fig. S2. As expected, octahedral  $\text{Cu}_2\text{O}$  microcrystals with  $\{111\}$  facets show a much higher photocatalytic activity than cubic. The absorption ability and photocatalytic activity of both octahedral and truncated octahedral  $\text{Cu}_2\text{O}$  particles are much higher than those of the other  $\text{Cu}_2\text{O}$  particles. The results suggest that octahedral  $\text{Cu}_2\text{O}$  particles formed entirely with  $\{111\}$  surfaces are more efficient for photocatalysis reactions than the particles of other morphologies containing partial  $\{100\}$  and  $\{110\}$  surfaces.<sup>22-25</sup> The TOC was used to further illuminate the photocatalytic ability of  $\text{Cu}_2\text{O}$  microcrystals. After irradiated 3 h, 60.1% of TOC was removed with octahedral  $\text{Cu}_2\text{O}$  microcrystals. Figure S3 are the SEM and TEM images of the octahedral and truncated octahedral  $\text{Cu}_2\text{O}$  microcrystals after the photocatalytic experiments (See Supporting Information), which show that the morphologies of  $\text{Cu}_2\text{O}$  microcrystals have no obvious change, compared with these before the photocatalytic experiment.

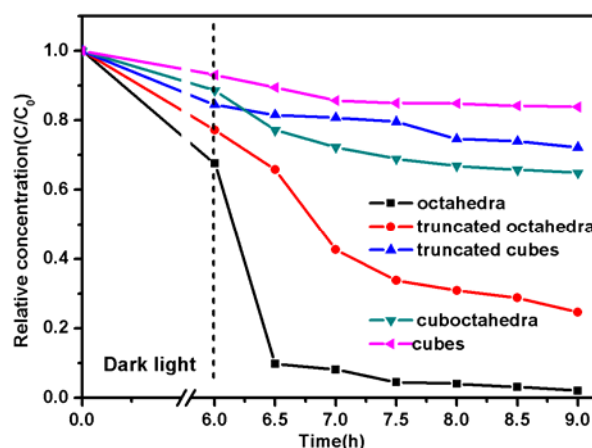


**Figure 4.** Extent of photodegradation of methylene orange (monitored at 455 nm) as a function of the irradiation time for the octahedra, truncated octahedra, truncated cubes, cuboctahedra and cubes, respectively.

## Conclusion

In conclusion, we reported a facile microwave-assisted heating technique for the synthesis of  $\text{Cu}_2\text{O}$  microcrystals with systematic shape evolution. Monodispersed octahedral, truncated octahedral, cuboctahedral, truncated cubic and cubic microcrystals were synthesized directly by varying the water/butyl alcohol ratio in the reaction medium. Due to the different dielectric losses of water and n-butyl alcohol, the heating efficiency of the reaction medium changed with the n-butyl alcohol/water volume ratio. The heating efficiency seemed to determine the growth rates of different crystal directions and thus affect the morphologies of  $\text{Cu}_2\text{O}$ . The absorption ability and photocatalytic activity of the

synthesized Cu<sub>2</sub>O microcrystals were investigated using MO dye as a model. The results demonstrate that both octahedral and truncated octahedral Cu<sub>2</sub>O particles have much higher activity than the other Cu<sub>2</sub>O particles. This investigation may provide a guidance for the shape-controlled synthesis of Cu<sub>2</sub>O microcrystals and also their application in the treatment of organic pollutants.

### Acknowledgements

This work was supported by the National Natural Science Foundation of China (No.21271082 and 21371068).

### References

- (1) Y. Xie, J. X. Huang, B. Li, Y. Liu and Y. T. Qian, *Adv. Mater.*, 2000, **12**, 1523.
- (2) J. T. Sampanthar and H. C. Zeng, *J. Am. Chem. Soc.*, 2002, **124**, 6668.
- (3) P. V. Braun, P. Osenar and S. I. Stupp, *Nature*, 1996, **380**, 325.
- (4) X. W. Lou and H. C. Zeng, *J. Am. Chem. Soc.*, 2003, **125**, 2697.
- (5) S. Iijima, *Nature*, 1991, **354**, 56.
- (6) P. C. Ohara, J. R. Heath and W. M. Gelbart, *Angew. Chem. Int. Ed. Engl.*, 1997, **36**, 1078.
- (7) A. P. Alivisatos, *Science*, 1996, **271**, 933.
- (8) M. A. El-Sayed, *Acc. Chem. Res.*, 2001, **34**, 257.
- (9) A. O. Musa, T. Akomolafe and M. J. Carter, *Sol. Energy Mater. Sol. Cells.*, 1998, **51**, 305.
- (10) J. T. Zhang, J. F. Liu, Q. Peng, X. Wang and Y. D. Li, *Chem. Mater.*, 2006, **18**, 867.
- (11) C. H. Kuo and M. H. Huang, *J. Am. Chem. Soc.*, 2008, **130**, 12815.
- (12) W. C. Huang, L. M. Lyu, Y. C. Yang and M. H. Huang, *J. Am. Chem. Soc.*, 2012, **134**, 1261.
- (13) J. Y. Ho and M. H. Huang, *J. Phys. Chem. C*, 2009, **113**, 14159.
- (14) C. H. Kuo, C. H. Chen and M. H. Huang, *Adv. Funct. Mater.*, 2007, **17**, 3773.
- (15) M. Leng, C. Yu and C. Wang, *CrystEngComm*, 2012, **14**, 8454.
- (16) P. Poizot, S. Laruelle, S. Grugeon, L. Dupont and J. M. Tarascon, *Nature*, 2000, **407**, 496.
- (17) M. J. Siegfried and K. S. Choi, *J. Am. Chem. Soc.*, 2006, **128**, 10356.
- (18) C. M. McShane and K. S. Choi, *J. Am. Chem. Soc.*, 2009, **131**, 2561.
- (19) M. J. Siegfried and K. S. Choi, *Angew. Chem. Int. Ed.*, 2005, **44**, 3218.
- (20) M. J. Siegfried and K. S. Choi, *Angew. Chem. Int. Ed.*, 2008, **47**, 368.
- (21) M. J. Siegfried and K. S. Choi, *Adv. Mater.*, 2004, **16**, 1743.
- (22) Y. M. Jiang, W. Y. Fu and H. B. Yang, *Cryst. Growth. Des.*, 2010, **10**, 99.
- (23) M. Poliakoff, J. M. Fitzpatrick, T. R. Farren and P. T. Anastas, *Science*, 2002, **297**, 807.
- (24) H. M. Yang, C. G. Huang, X. H. Su and A.D. Tang, *J. Alloys Compd.*, 2005, **402**, 274.
- (25) Y. Zhao, J. M. Hong and J. J. Zhu, *J. Cryst. Growth.*, 2004, **270**, 438.
- (26) M. N. Nadagouda and R. S. Varma, *Cryst. Growth Des.*, 2007, **8**, 291.
- (27) Y. He, L. M. Sai, H. T. Lu, M. Hu, W. Y. Lai, Q. L. Fan, L. H. Wang and W. Huang, *Chem. Mater.*, 2007, **19**, 359.
- (28) A.B. Panda, G. Glaspell and M. S. El-Shall, *J. Phys. Chem. C*, 2007, **111**, 1861.
- (29) Y. Jiang, Y. J. Zhu and G. F. Cheng, *Cryst. Growth Des.*, 2006, **6**, 2174.
- (30) I. Bilecka and M. Niederberger, *Chimia*, 2009, **63**, 581.
- (31) I. Bilecka and M. Niederberger, *Nanoscale*, 2010, **2**, 1358.
- (32) G. R. Patzke, Y. Zhou, R. Kontic and F. Conrad, *Angew. Chem.*, 2011, **123**, 852.
- (33) L. Vayssieres and M. Graetzel, *Angew. Chem.*, 2004, **116**, 3752.
- (34) J. Zhang, H. Liu, Z. Wang, N. Ming, Z. Li and A. S. Biris, *Adv. Funct. Mater.*, 2007, **17**, 3897.
- (35) C. Gabriel, S. Gabriel, E. H. Grant, B. S. Halstead and D. M. P. Mingos, *Chem. Soc. Rev.*, 1998, **27**, 213.
- (36) D. M. P. Mingos and D. R. Baghurst, *Chem. Soc. Rev.*, 1991, **20**, 1.
- (37) W. B. Floriano and M. A. C. Nascimento, *Braz. J. Phys.*, 2004, **34**, 38.
- (38) M. H. Kim, B. K. Lim, E. P. Lee and Y. N. Xia, *J. Mater. Chem.*, 2008, **18**, 4069.
- (39) Z. L. Wang, *J. Phys. Chem. B*, 2000, **104**, 1153.